

Irreversibility and correlations in coupled quantum oscillators

M. Brunelli¹ and M. Paternostro¹

¹*Centre for Theoretical Atomic, Molecular and Optical Physics,
School of Mathematics and Physics, Queen's University, Belfast BT7 1NN, United Kingdom*

We investigate the link between the irreversibility generated by a stationary dissipative process and the correlations established within a composite quantum system. We provide two equivalent expressions for the entropy generated in the non-equilibrium steady state of coupled quantum harmonic oscillators that allow for a simple interpretation of the onset of irreversibility. We then unveil a quantitative relation between the entropy production rate and correlations, both total and quantum, built between the two oscillators. In the small-coupling limit, the entropy production rate is shown to be proportional to both the mutual information and the quantum correlations. We apply our results to the analysis of the optomechanical interaction between a nano-mechanical resonator and a cavity field, and show that the behavior of the entropy production captures the peculiar features of the model, such as sideband cooling and amplification.

The quantum-limited control of systems trespassing the microscopic domain requires a quantitative assessment of the irreversibility generated during their evolution. Realistic transformations in composite quantum systems take place at a finite rate, thus departing from the quasi-static limit, and unavoidably involve the interaction with the surroundings. Both these features bring about irreversibility, which is typically manifested by the generation of entropy and the dissipation of heat into the environment [1]. However, despite being of primary importance, entropy production remains an elusive quantity, often inaccessible to direct probing. This is a particularly delicate point when applying thermodynamic considerations. Indeed, failing to properly take into account all the mechanisms responsible for dissipation (not known *a priori*) determines an underestimation of the entropy production [2]. This can lead to erroneous conclusions, for instance in the characterization of the efficiency of recently proposed quantum thermal machines and engines [3].

Another defining feature of composite systems is that correlations may be shared among their constituents. In real-life scenarios, correlations are typically established as the result of some dynamical process which modifies the energetic and entropic balance of the system. The building-up of correlations within a quantum system must then be accompanied by the production of entropy. In turn, this implies that irreversibility and correlations cannot be tackled separately.

In this paper, we carry out a detailed study of the irreversibility generated in the stationary state of a bipartite quantum system. We consider a simple system that yet encapsulates most of the salient features encountered in quantum-controlled experiments, consisting of two linearly interacting quantum oscillators, each dissipating into a local bath. We derive two equivalent expressions for the rate of irreversible entropy production at the steady state, linking the irreversibility to either the number of excitations stored in the two modes (with respect to their equilibrium values) or the correlations between their motion, thus providing a clear picture of the onset of irreversibility.

At variance with standard approaches, we investigate the entropic cost of establishing correlations in a realistic finite-time process. We compare the behavior of the entropy production to the total correlations and the quantum ones, quantified by the mutual information and the discord, respectively [4, 5]. We find that the former behaves monotonically with respect to the latter quantities. In particular, when the coupling between the systems is small compared to their natural frequencies, we find simple proportionality relations between the entropy production and either the mutual information or the quantum discord. In Ref. [6] the thermodynamic cost of establishing correlations has been addressed from a purely information-theoretical point of view, without addressing their dynamical origin. On the contrary, our analysis shows explicitly that generation of correlations and production of entropy are complementary aspects in a dissipative process. We apply our results to the characterization of irreversibility in an optomechanical system [7]. We show how the behavior of the entropy production fully accounts for the salient features of the system in different regimes, e.g. cavity-mediated cooling and amplification of the mechanical resonator.

Our results suggest that irreversibility and correlations are two sides of the same coin: as expected, generation of correlations, both classical and quantum, comes at the price of increasing the entropy of the system plus environment. Likewise, irreversibility in composite quantum systems, very much like correlations, can be viewed as a resource. Harness irreversible dynamics in a controllable way can be beneficial for quantum information processing, as we quantitatively assess.

The remainder of this work is organized as follows: In Sec. I we introduce the model and derive the expressions of the entropy production upon which our analysis relies. Sec. II discusses in detail the features of the entropy production. In Sec. III we first define correlation measures based on the Rényi-2 entropy, which are instrumental to highlight the link between entropy production and correlations, and then present a detailed analysis of such a connection. In Sec. IV, our results are specialized to the relevant case of an optomechanical system. Sec. V draws

our conclusions and sketches the questions that are left open by our study. Finally, a set of four Appendices presents the most technical parts of our work.

I. IRREVERSIBILITY IN COUPLED QUANTUM OSCILLATORS

The second law of thermodynamics, when referred to a system that exchanges energy with its surroundings, takes the familiar form [8]

$$\Delta S \geq \int \frac{\delta Q}{T}, \quad (1)$$

where δQ is the infinitesimal heat absorbed by the system. The strict inequality characterizes irreversible processes for which some energy is dissipated in the form of heat and lost into the environment [9]. Eq. (1) can be cast into an equality by highlighting the nonnegative mismatch and, for convenience, expressed in terms of rates, so that one finally has

$$\frac{dS}{dt} = \Phi(t) + \Pi(t), \quad (2)$$

where $\Pi(t)$ is the *irreversible entropy production rate* and $\Phi(t)$ is the entropy flux from the environment into the system. When the system attains a stationary state, such quantities take values Π_s and Φ_s respectively, so that $\Pi_s = -\Phi_s > 0$, while only when both terms vanish one recovers thermal equilibrium. The entropy production rate thus accounts for the irreversibility of any physical process and represents a key quantity for the characterization of finite-time transformations and the performances of thermal machines.

Several characterizations of entropy production have been given, especially in the framework of stochastic thermodynamics. In such a context it has been shown that the entropy production rate originates from the temporal-symmetry breaking at the level of single trajectories [2, 12, 13] and satisfies a fluctuation theorem [14], from which one can deduce its average non-negativity. In some limit, these conclusions have also been extended to open quantum systems [15, 16]. Interestingly, in Ref. [17] a characterization of entropy production as correlation between a system and a reservoir has been put forward, which is somehow close in spirit to our investigation. However, although entropy production is formally well characterized, given its full dependence on the microscopic trajectory of the system, few useful expressions for cases at hand are available and it remains an elusive quantity to measure, with just a handful of experimental measurements reported in literature [18–20]. Recently a first measurement of the entropy production rate in driven-dissipative quantum systems has been reported [21]. The rate of irreversible entropy production, as specified by Eq. (2), is the main tool of our investigation, which we exploit to assess the irreversibility in the open dynamics of a bipartite quantum system.

We consider two quantum oscillators described by the field operators \hat{a} and \hat{b} , having frequencies $\omega_{a,b}$ and masses $m_{a,b}$. The two oscillators are linearly coupled with strength G , so that the interacting system is described by

$$\hat{H} = \frac{\hbar\omega_a}{2}(\hat{q}_a^2 + \hat{p}_a^2) + \frac{\hbar\omega_b}{2}(\hat{q}_b^2 + \hat{p}_b^2) + \hbar G\hat{q}_a\hat{q}_b, \quad (3)$$

where $\hat{q}_{a,b}$ and $\hat{p}_{a,b}$ are dimensionless position and momentum operators. The system is also interacting with its surroundings, which we model as two independent Markovian baths at temperature $T_{a,b}$ so that, at equilibrium, the two oscillators have an average number of excitations $N_{a,b} = (e^{\hbar\omega_{a,b}/k_B T_{a,b}} - 1)^{-1}$. The baths are assumed to be mutually independent. The system is then subjected to extra quantum noise, described by the input operators \hat{a}^{in} , \hat{b}^{in} satisfying $\langle \hat{a}^{\text{in},\dagger}(t)\hat{a}^{\text{in}}(t') \rangle = N_a\delta(t-t')$, and $\langle \hat{a}^{\text{in}}(t)\hat{a}^{\text{in},\dagger}(t') \rangle = (N_a + 1)\delta(t-t')$ (similar expressions hold for \hat{b}^{in}). Finally, the dissipation to the local baths occurs with rates $\kappa_{a,b}$. A broad range of systems fall into this description, ranging from quantum optics to solid-state devices, condensates and atomic ensembles. The resulting open dynamics can be described by the quantum Langevin equation $\dot{\hat{u}} = A\hat{u}(t) + \hat{N}(t)$ for the vector of the dimensionless quadrature operators $\hat{u} = (\hat{q}_a, \hat{p}_a, \hat{q}_b, \hat{p}_b)^T$, where the drift matrix A is given by

$$A = \begin{pmatrix} -\kappa_a & \omega_a & 0 & 0 \\ -\omega_a & -\kappa_a & G & 0 \\ 0 & 0 & -\kappa_b & \omega_b \\ G & 0 & -\omega_b & -\kappa_b \end{pmatrix}, \quad (4)$$

while the noise vector is $\hat{N} = (\sqrt{2\kappa_a}\hat{q}_a^{\text{in}}, \sqrt{2\kappa_a}\hat{p}_a^{\text{in}}, \sqrt{2\kappa_b}\hat{q}_b^{\text{in}}, \sqrt{2\kappa_b}\hat{p}_b^{\text{in}})^T$. The linear character of the dynamics, together with the choice of initial Gaussian states, implies that the probability distribution describing the two oscillators is Gaussian at any time [22, 23]. Therefore a complete description of the system is given in terms of the second statistical moments of the quadrature operators, which can be arranged in the covariance matrix σ of entries $\sigma_{ij} := \langle \{\hat{u}_i(t), \hat{u}_j(t)\} \rangle / 2 - \langle \hat{u}_i(t) \rangle \langle \hat{u}_j(t) \rangle$. The first moments can straightforwardly be made null by a suitable displacement in the phase space and we assume, from now on, that this is indeed the case. The equation of motion for the covariance matrix reads

$$\dot{\sigma} = A\sigma + \sigma A^T + D, \quad (5)$$

where the diffusion matrix is given by $D = (1 + 2N_a)\kappa_a\mathbb{1}_a \oplus (1 + 2N_b)\kappa_b\mathbb{1}_b$.

The competition between the two baths at different temperatures causes the breaking of the detailed balance and brings the system out of equilibrium [12]. Moreover, the unitary evolution generated by Eq. (3) does not commute with the dissipative part of the dynamics. Therefore, the coherent coupling between the quantum oscillators affects the overall irreversibility. We assume the

system to be always stable, in such a way that a unique non-equilibrium steady state, described by the stationary covariance matrix σ_s such that $A\sigma_s + \sigma_s A^T = -D$, is eventually attained.

The open dynamics can be described in terms of Fokker-Plank equations for the Wigner function of the joint system and, provided that the symmetry of the variables under time-reversal is explicitly taken into account [24–26], an analytical expression for Π_s can be derived starting from Eq. (2). Explicit calculations shown in Appendix B lead to the following simple expression for the stationary rate of entropy production

$$\Pi_s = 2\kappa_a \left(\frac{\langle \hat{q}_a^2 \rangle_s + \langle \hat{p}_a^2 \rangle_s}{2N_a + 1} - 1 \right) + 2\kappa_b \left(\frac{\langle \hat{q}_b^2 \rangle_s + \langle \hat{p}_b^2 \rangle_s}{2N_b + 1} - 1 \right), \quad (6)$$

where $\langle \cdot \rangle_s$ specifies that the expectation values are taken at the stationary state. Since the first (second) term depends only on quantities labeled by a (b) we dub it contribution a (b) to the entropy production rate and call it μ_a (μ_b). We thus have

$$\mu_k = 2\kappa_k \left(\frac{N_{k,s} + 1/2}{N_k + 1/2} - 1 \right), \quad (k = a, b) \quad (7)$$

where we set $N_{a,s} = \langle \hat{a}^\dagger \hat{a} \rangle_s$ and $N_a = \langle \hat{a}^\dagger \hat{a} \rangle_{\text{eq}}$, and similarly for μ_b . The main feature of Eq. (7) is that it links the irreversibility generated by the stationary process to the change in the amount of excitations carried by each oscillator with respect to the equilibrium value, thus expressing production of entropy in very simple terms.

If the system is noninteracting, each oscillator equilibrates with its own bath and from Eq. (7) we see that Π_s identically vanishes. Second, as $\Pi_s = \mu_a + \mu_b \geq 0$, from Eq. (7) we conclude that no process leading at the same time to $N_{a,s} < N_a$ and $N_{b,s} < N_b$ can occur: the thermodynamic arrow of time is translated in a constraint on the final occupations of the two oscillators. An instance of forbidden process is sketched in Fig. 1 (a). However, nothing prevents a local reduction of entropy, e.g. $\mu_b < 0$ as shown in panel (b), as long as it is (over)compensated by an increase of the other contribution $\mu_a > -\mu_b$. Such condition entails $N_{b,s} < N_b$ and thus corresponds to the cooling one oscillator assisted by the interaction. This also implies that, singularly taken, neither μ_a nor μ_b can be interpreted as an entropy production.

Looking at Eq. (6) we notice that there is no explicit dependence of Π_s on the off-diagonal elements of the covariance matrix. Correlations between the two modes are hidden in the full expression of the expectation values. It would be desirable to have an alternative form for $\mu_{a,b}$, where the role of the correlations established at the steady state is made explicit. Such an expression can actually be derived (calculations are reported in Appendix C) and is given by

$$\mu_a = \frac{G}{N_a + 1/2} \langle \hat{p}_a \hat{q}_b \rangle_s, \quad \mu_b = \frac{G}{N_b + 1/2} \langle \hat{q}_a \hat{p}_b \rangle_s, \quad (8)$$

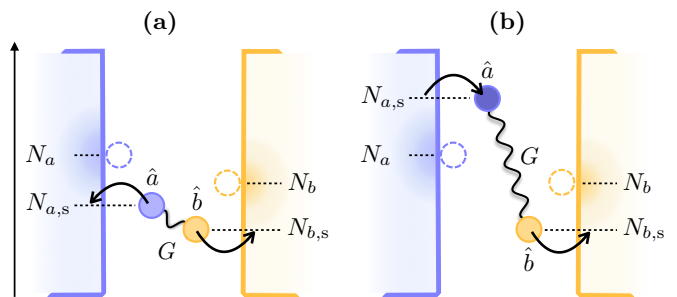


FIG. 1. The oscillators corresponding to modes \hat{a} (blue) and \hat{b} (yellow) are initially in thermal equilibrium with a number of excitations N_a and N_b , respectively (dashed circles). By switching on the coupling G they reach a stationary state characterized by occupations $N_{a,s}$ and $N_{b,s}$ (full circles). (a): Example of a forbidden stationary process where both occupations decrease with respect their equilibrium values, thus leading to $\Pi_s < 0$. (b): Entropy can still locally decrease ($\mu_b < 0$) as a consequence of a reduction in the excitations $N_{b,s} < N_b$, but this necessitates excitations to be accumulated in mode \hat{a} (darker blue circle).

where we have $\langle \hat{p}_a \hat{q}_b \rangle_s = [\sigma_s]_{23}$ and $\langle \hat{q}_a \hat{p}_b \rangle_s = [\sigma_s]_{14}$. From Eq. (8), we explicitly see that Π_s vanishes for uncoupled systems, since each oscillator independently equilibrates with its own bath. Eq. (8) links in a quantitative way the irreversibility of the transformation with some correlation function of the dynamical variables. The link between the entropy production and the correlations shared by the oscillators will be further explored in Sec. III, where the amount of total and quantum correlations is quantified.

II. ANALYSIS OF THE STATIONARY ENTROPY PRODUCTION RATE

In this Section we give a full account of the behavior of the stationary entropy production. For the sake of convenience, all the frequencies have been rescaled by ω_b , so that we deal with dimensionless quantities. However, in order to avoid redundancies, the rescaling will be omitted and the same notation kept, except from the figures and the related captions, where the relevant quantities are explicitly shown in units of ω_b .

In Fig. 2 we show the stationary entropy production rate Π_s , together with its components $\mu_{a,b}$, against the rescaled frequency ω_a . In panels (a)-(c) the reservoirs are in the ground state ($N_a = N_b = 0$) and we see that μ_a and μ_b are both positive and very similar (although not equal). This is because the steady-state occupations can only increase with respect to their initial value and, by looking at Eq. (7), so must the entropy. If we then consider some initial thermal occupation in one oscillator, as shown in Fig. 2 (d)-(f) for the case $N_b > 0$, we see that $\Pi_s \approx \mu_a$, featuring a distinctive peak at $\omega_a = 1$. Correspondingly, μ_b displays a negative dip. The signifi-

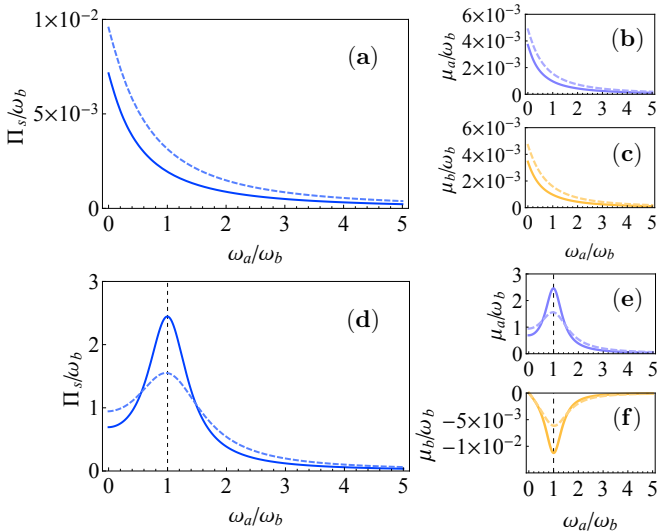


FIG. 2. Entropy production rate Π_s/ω_b (a) and its two contributions μ_a/ω_b (b) and μ_b/ω_b (c) against the ratio of the two frequencies; solid curves correspond to $\kappa_a = \kappa_b = 0.2\omega_b$, while dashed ones to $\kappa_a = 0.2\omega_b$ and $\kappa_b = 0.5\omega_b$. Other parameters are $N_a = N_b = 0$ and $G = 0.1\omega_b$. Panels (d), (e), (f) represent the same plots as (a), (b), (c) when introducing an imbalance in thermal excitations $N_a = 0$ and $N_b = 100$.

cant difference in magnitude between μ_a and μ_b ensures the overall positivity of Π_s . By comparing panels (a) and (d) we immediately notice that the introduction of some imbalance between the initial populations of the oscillators causes Π_s to grow, thus witnessing irreversibility due to transport, since the coupled oscillators now mediate a net heat flux between the two baths. Moreover, in light of Eq. (7), a steady negative value of μ_b implies a reduction of steady excitations $N_{b,s} < N_b$ and thus an effective cooling of oscillator b (as sketched in Fig. 1, right panel). The maximum (minimum) assumed by μ_a (μ_b) at $\omega_a = 1$, namely when the oscillators have identical frequencies, can be understood as follows. For $\omega_a \approx 1$, and provided that $G < \omega_a$, we can move to the rotating frame and apply the rotating-wave approximation, so that the interaction Hamiltonian takes the form $H_I \propto \hat{a}^\dagger \hat{b} + \hat{a} \hat{b}^\dagger$. The latter is a pure exchange interaction and hence is

optimal for heat transfer, thus explaining why the degree of irreversibility is large [27]. These features will be discussed in more detail in Sec. IV when addressing the cavity-assisted cooling of a mechanical resonator. On the other hand, from Fig. 2 we see that Π_s tends to zero for $\omega_a \gg 1$. This is because when the oscillators are far-off resonance they are effectively decoupled, so that each of them thermalizes to its own bath. Finally, we can also inspect the role played by the dissipation rates $\kappa_{a,b}$ on the irreversible entropy production. The solid curves in the plots correspond to identical loss rates $\kappa_a = \kappa_b$ while the dashed curves refer to the case of different values ($\kappa_a = 0.2, \kappa_b = 0.5$), and we can see that a general feature is the broadening of Π_s with the losses. When the temperature $T_{a,b}$ of the baths and the frequencies $\omega_{a,b}$ are such that the initial number of thermal excitations is the same, i.e. $N_a = N_b = N$, the entropy production rate turns out to be independent on N , which is a clear feature of the enforced symmetry between the two subsystems. Also, from Fig. 3 we see that Π_s achieves its minimum for $N_a = N_b$, while when N_b exceeds N_a , Π_s grows linearly with respect to N_b , i.e. proportionally to the imbalance in populations. For $N_b/N_a < 1$ we see an abrupt increase in the entropy production rate, which however remains finite for $N_b = 0$.

Some more quantitative insight can be gathered in the small coupling limit, after expanding $\mu_{a,b}$ in power series of G , getting the following expressions

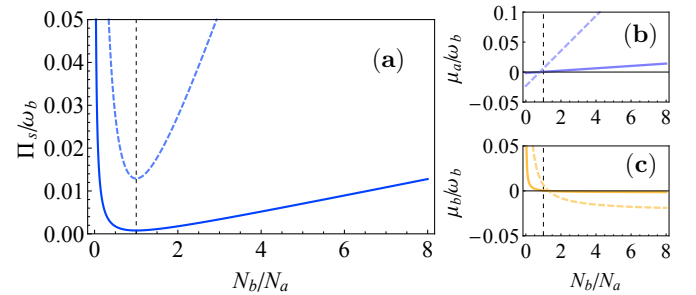


FIG. 3. Entropy production rate Π_s/ω_b (a) and its two contributions μ_a/ω_b (b) and μ_b/ω_b (c) against the ratio N_b/N_a . The oscillators have the same frequency $\omega_a = \omega_b$, $\kappa_a = 0.2\omega_b$ and $\kappa_b = 0.5\omega_b$, and either coupled with strength $G = 0.05\omega_b$ (solid curves) or $G = 0.2\omega_b$ (dashed curves).

$$\mu_a = \frac{G^2 \kappa_{\text{tot}} [1 + \kappa_{\text{tot}}^2 + \omega_a^2 - 2\omega_a(2N_a + 1) + 2N_b(1 + \kappa_{\text{tot}}^2 + \omega_a^2)]}{(2N_a + 1) [2\omega_a^2(\kappa_{\text{tot}}^2 - 1) + (\kappa_{\text{tot}}^2 + 1)^2 + \omega_a^4]} + \mathcal{O}(G^4),$$

$$\mu_b = \frac{G^2 \kappa_{\text{tot}} [1 + \kappa_{\text{tot}}^2 + \omega_a^2 - 2\omega_a(2N_b + 1) + 2N_a(1 + \kappa_{\text{tot}}^2 + \omega_a^2)]}{(2N_b + 1) [2\omega_a^2(\kappa_{\text{tot}}^2 - 1) + (\kappa_{\text{tot}}^2 + 1)^2 + \omega_a^4]} + \mathcal{O}(G^4),$$

where we set $\kappa_{\text{tot}} = \kappa_a + \kappa_b$. We can see that the first

non vanishing term is quadratic in G , and in addition it

can be checked that μ_k ($k = a, b$) is an even function of G . We also notice that in such a small coupling regime, μ_a and μ_b are simply related to each other by the swap of the thermal excitations $N_{a,b}$: the imbalance between N_a and N_b has a clear effect on the two components $\mu_{a,b}$ and dictates which of the oscillators will reduce its local entropy and which one will compensate. The coherent coupling between the two oscillators alters this simple picture, since already by including the fourth-order term this ceases to be true. If we then expand $\mu_{a,b}$ for large values of ω_a , we obtain the following expressions for the asymptotic behavior of the tails

$$\begin{aligned}\mu_a &= \frac{1}{\omega_a^2} \frac{G^2 \kappa_{\text{tot}} (1 + 2N_b)}{1 + 2N_a} + \mathcal{O}\left(\frac{1}{\omega_a^3}\right), \\ \mu_b &= \frac{1}{\omega_a^2} \left[\frac{G^2 \kappa_{\text{tot}} (1 + 2N_a)}{1 + 2N_b} + \frac{G^4 \kappa_b}{2(\kappa_b^2 + 1)} \right] + \mathcal{O}\left(\frac{1}{\omega_a^3}\right).\end{aligned}\quad (10)$$

For large values of ω_a , the entropy production rate (at the leading order) decays as ω_a^{-2} . In the small-coupling limit, when the term proportional to G^4 in Eq. (10) can be neglected, $\mu_{a,b}$ can be mapped into each other by swapping the thermal excitations, as previously argued. Finally, we notice that both contributions in Eq. (10) are strictly positive, which may seem in contradiction to what shown in Fig. 2 (f), where μ_b takes negative values. However, if we retained the next-order term in the expansion, we would find that μ_b approaches zero from below for $\omega_a \gg 1$, in agreement with the plot.

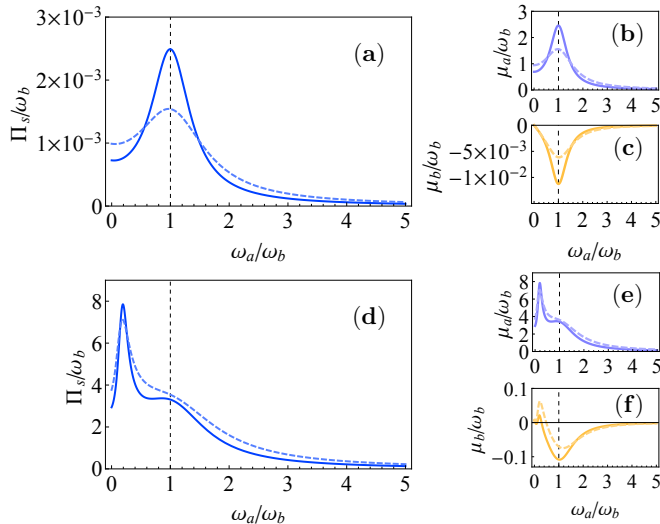


FIG. 4. We plot Π_s/ω_b [panel (a)], μ_a/ω_b [panel (b)] and μ_b/ω_b [panel (c)] against the ratio of the two frequencies for different values of the coupling; solid lines correspond to $\kappa_{a,b} = 0.2\omega_b$, while dashed ones to $\kappa_a = 0.2\omega_b$ and $\kappa_b = 0.5\omega_b$. Other parameters are $N_a = 0$, $N_b = 10$ and $G = 0.01\omega_b$. Panels (d)-(f) show the same plots as panels (a)-(c) but for $G = 0.6\omega_b$.

We conclude the description of the features of Π_s by inspecting its dependence on the coupling strength G .

By comparing Fig. 4 (a), corresponding to $G = 0.01$, with Fig. 2 (d), which is for $G = 0.1$, we further confirm the quadratic scaling in Eq. (9), since Π_s retains the very same shape but drops by two orders of magnitude. On the other hand, in Fig. 4 (d) we show an instance of the strong coupling regime, where the strength of the coherent coupling exceeds the dissipation rates and is comparable with the oscillation frequencies. Now, Π_s exhibits a second peak, which is a clear signature of hybridization.

A. Identical oscillators and identical baths

If the baths have the same temperature T and the oscillators the same frequency ω , which results in the same number of excitations $N = (e^{\hbar\omega/k_B T} - 1)^{-1}$, we can directly relate the entropy production rate to a single element of the covariance matrix of the oscillators' state. We refer to the entropy production rate in this case as $\tilde{\Pi}_s$, whose expression is given by $\tilde{\Pi}_s = \frac{G}{\omega} \frac{\kappa_{\text{tot}}}{N+1/2} \langle \hat{q}_a \hat{q}_b \rangle_s$, which shows an explicit proportionality to the matrix element $\langle \hat{q}_a \hat{q}_b \rangle_s = [\sigma_s]_{13}$. By using the explicit form of such covariance matrix entry, we have

$$\tilde{\Pi}_s = \frac{G^2 \kappa_{\text{tot}} [G^2 (\kappa_{\text{tot}}^2 - 3\kappa_a \kappa_b + 1) + 4\kappa_a \kappa_b \chi_{ab}]}{2(\chi_{ab} - G^2) [G^2 + \kappa_a \kappa_b (\kappa_{\text{tot}}^2 + 4)]}, \quad (11)$$

where we have set $\chi_{ab} = (\kappa_a^2 + 1)(\kappa_b^2 + 1)$. Eq. (11) shows that, in agreement with what previously stated, for two identical oscillators in the absence of any thermal gradient, the entropy production is independent of N . Furthermore, if we impose $\kappa_a = \kappa_b = \kappa$ (and dub the corresponding entropy production $\tilde{\Pi}_\kappa$) we obtain the simple expression

$$\tilde{\Pi}_\kappa = \frac{G^2 \kappa (\kappa^2 + 1)}{(\kappa^2 + 1)^2 - G^2}. \quad (12)$$

Having two identical oscillators dissipating at the same rate into identical baths, the open system is in its most symmetric configuration, and the resulting stationary state is the closest possible to equilibrium. Accordingly, one can verify that in this scenario the entropy production is minimised. Moreover, a detailed calculation shows that, in this case, the oscillators contribute equally to the production of entropy, i.e., $\tilde{\mu}_a = \tilde{\mu}_b = \tilde{\Pi}_\kappa/2$.

III. ENTROPY PRODUCTION RATE, TOTAL AND QUANTUM CORRELATIONS

A. Quantifying correlation via the Rényi-2 entropy

The mutual information $\mathcal{I}(\varrho_{a:b}) = S(\varrho_a) + S(\varrho_b) - S(\varrho_{ab})$ quantifies the total amount of correlations shared by two systems, the rationale being that only when two systems are completely uncorrelated their joint entropy equals the sum of the reduced entropies [28]. While the

standard way to quantify entropy is to use the von Neumann entropy, the Gaussian nature of the states at hand here, which are completely characterized by the two-mode covariance matrix

$$\sigma_{ab} = \begin{pmatrix} \sigma_a & c_{ab} \\ c_{ab}^T & \sigma_b \end{pmatrix}, \quad (13)$$

legitimizes the use of another expression for the entropy. This is given in terms of the Shannon entropy of the Wigner distribution $\mathcal{W}(\sigma_{ab}) = e^{-u^T \sigma_{ab}^{-1} u/2} / (\pi^2 \sqrt{\det \sigma_{ab}})$, and reads

$$S(\sigma_{ab}) = \int_{\mathbb{R}^4} d^4 u \mathcal{W}(\sigma_{ab}) \log \mathcal{W}(\sigma_{ab}), \quad (14)$$

where $u = (q_a, p_a, q_b, p_b)^T$ is the vector of phase-space variables. For Gaussian distributions the expression can be easily evaluated and gives

$$S(\sigma_{ab}) = \frac{1}{2} \log(\det \sigma_{ab}). \quad (15)$$

Ref. [29] pointed out that $S(\sigma_{ab})$ coincides (up to an additive constant) with the generalized Rényi entropy of order 2, $S_2(\varrho) = -\log \text{Tr} [\varrho^2]$, and proved that it enjoys all the properties required to be a legitimate entropy measure, such as strong subadditivity. Such a correspondence is discussed in detail in Appendix A.

We can then define the mutual information as $\mathcal{I}(\sigma_{a:b}) = S(\sigma_{ab} || \sigma_a \oplus \sigma_b)$, namely as the Kullback-Leibler divergence between the Wigner function of the joint state and the product of those associated with the reduced ones. From Eq. (15) it immediately follows that

$$\mathcal{I}(\sigma_{a:b}) = \frac{1}{2} \log \left(\frac{\det \sigma_{ab}}{\det \sigma_a \det \sigma_b} \right). \quad (16)$$

Finally, also the amount of quantum correlations between the two modes can be expressed in terms of the Rényi-2 entropy. The quantum discord (with respect to measurements made on mode \hat{b}) is defined as the difference

$$\mathcal{D}(\sigma_{a|b}) = \mathcal{I}(\sigma_{a:b}) - \mathcal{J}(\sigma_{a|b}), \quad (17)$$

between the mutual information $\mathcal{I}(\sigma_{a:b})$ and the one-way classical correlations $\mathcal{J}(\sigma_{a|b}) = \sup_{\pi_b(X)} \{S(\sigma_a) - \int dX p_X S(\sigma_{a|X}^{\pi_b})\}$, where the maximization is taken over all the possible measurements $\hat{\pi}_b(X) \geq 0$ such that $\int dX \hat{\pi}_b(X) = \mathbb{1}_b$, implemented on \hat{b} . If we restrict our attention to Gaussian measurements, we can rewrite Eq. (17) as $\mathcal{D}(\sigma_{a|b}) = S(\sigma_b) - S(\sigma_{ab}) + \inf_{\pi_b} S(\sigma_a^{\pi_b})$, and the minimization can be performed analytically. All the details are reported in Appendix D, together with the fully-fledge expression of $\mathcal{D}(\sigma_{a|b})$. In what follows we will employ such figures of merit to characterize the correlations between the two modes \hat{a} and \hat{b} at the stationary state. When no further specifications are needed, we will refer to the Rényi-2 mutual information and discord simply as \mathcal{I} and \mathcal{D} , respectively.

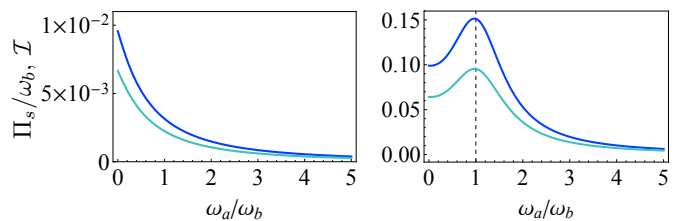


FIG. 5. Comparison between the rescaled entropy production rate Π_s/ω_b (blue), the mutual information \mathcal{I} (green) and the quantum discord \mathcal{D} (magenta) as a function of the ratio of the two frequencies ω_a/ω_b , for $G = 0.1\omega_b$, $\kappa_a = 0.2\omega_b$, $\kappa_b = 0.5\omega_b$, $N_a = 0$ and either $N_b = 0$ (left) or $N_b = 10$ (right).

B. Relationship between entropy production rate and mutual information

The full expression for the mutual information between the two oscillators at the steady state is extremely involved, and it will not be reported here. However, we must stress that in general its form bears no resemblance with the entropy production rate: Π_s is a rational function, and in particular the ratio between two fourth order polynomials in G , while from Eq. (16) we clearly see that \mathcal{I} is logarithmic. Furthermore, at variance with Π_s , the mutual information cannot be reduced to the sum of two separate contributions, each ascribable to a single oscillator. These facts reflect the different origin of the two terms. On the other hand, thanks to Eq. (8) we know that Π_s is explicitly linked to position-momentum correlations among the oscillators, so that one may wonder about a possible connection between the rate of entropy produced and the correlations present within the system. In fact, by comparing Π_s and \mathcal{I} , as done in Fig. 5, we notice a striking similarity: despite their different functional form, \mathcal{I} is clearly a one-to-one function of Π_s . This represents a first evidence that the irreversibility generated by the stationary process and the total amount of correlations shared between the two modes are tightly related.

When the oscillators are uncoupled or far-off-resonance, and thus effectively decoupled, they separately reach thermal equilibrium and the total state of the system consists of locally thermal states, yielding vanishing values of both Π_s and \mathcal{I} . Another remarkable feature shared by the two figures of merit is that, when the number of thermal excitations $N_a = N_b = N$ is the same, both \mathcal{I} and Π_s turn out to be independent on N . As one can imagine, this is however not the case for the amount of entanglement, if any, shared by the two oscillators, which crucially depends on the thermal occupations and is rapidly depleted when increasing $N_{a,b}$ (even for $N_a = N_b = N$). In Fig. 6 (b) we computed the logarithmic negativity when both oscillators dissipate into the vacuum ($N = 0$); if we raised the thermal excitations to $N = 1$ we would find Π_s and \mathcal{I} unchanged but the entanglement completely spoiled. Actually, as shown

in panel (c), already lifting one of the two thermal occupation numbers ($N_b = 1$) causes a complete loss of the entanglement (notice however that Π_s increases thanks to the introduction of a thermal gradient). Furthermore, as we can appreciate from Fig. 6 (b) and (c), by increasing the coupling strength G the agreement between the two figures of merit gets worse. For big imbalances in the initial thermal populations and strong couplings \mathcal{I} and Π_s can develop different features and in some instance also the qualitative agreement may be lost.

In order to gain a more quantitative understanding about the connection highlighted in Fig. 5 we can expand both Π_s and \mathcal{I} in power series of G [for Π_s this amount to take the sum of the expansions of $\mu_{a,b}$ in Eq. (9)], obtaining the following simple relation

$$\mathcal{I} = \frac{\Pi_s}{2\kappa_{\text{tot}}} + \mathcal{O}(G^4). \quad (18)$$

Eq. (18) is one of our main results, since it establishes a *proportionality between the total amount of correlations and the irreversibility of the dissipative process*. Provided that the coupling strength is not too big with respect to the frequency ω_b , \mathcal{I} and Π_s turn out to be two sides of the same coin: more correlations in the system come at the price of an increased irreversibility and, conversely, the amount of entropy generated by the dissipative process is proportional to the correlations established by it. We must stress that this expansion does not necessarily entails a classical-like limit, and also systems displaying pronounced quantum features, e.g. stationary entangled states of the two oscillators, fulfill Eq. (18), as further discussed in the next Section.

Finally, for the particular case of two identical oscillators dissipating with the same rate κ into baths at the same temperature T , the mutual information \mathcal{I} takes the form

$$\tilde{\mathcal{I}}_\kappa = \frac{1}{2} \log \left[\frac{4(G^2 K_- + 2K_+^2)^2}{(K_+^2 - G^2)(G^4 + 8G^2 K_- + 16K_+^2)} \right], \quad (19)$$

where we set $K_\pm = \kappa^2 \pm 1$. The corresponding expression of the entropy production rate has been given in Eq. (12). Eq. (19) is an exact result, valid for any value of the coupling strength, independent on N . By comparing Eqs. (12) and Eq. (19) we can conclude that, even for the specific case examined, their full expressions bear little resemblance.

C. Relationship between entropy production rate and quantum discord

We can also investigate the relation between Π_s and the amount of quantum correlations, as quantified by the Rényi-2 discord \mathcal{D} , shared by the two oscillators at the steady state. From Fig. 6 we see how the discord, which corresponds to the magenta curve, although assuming lower values, shares some common feature with Π_s . In

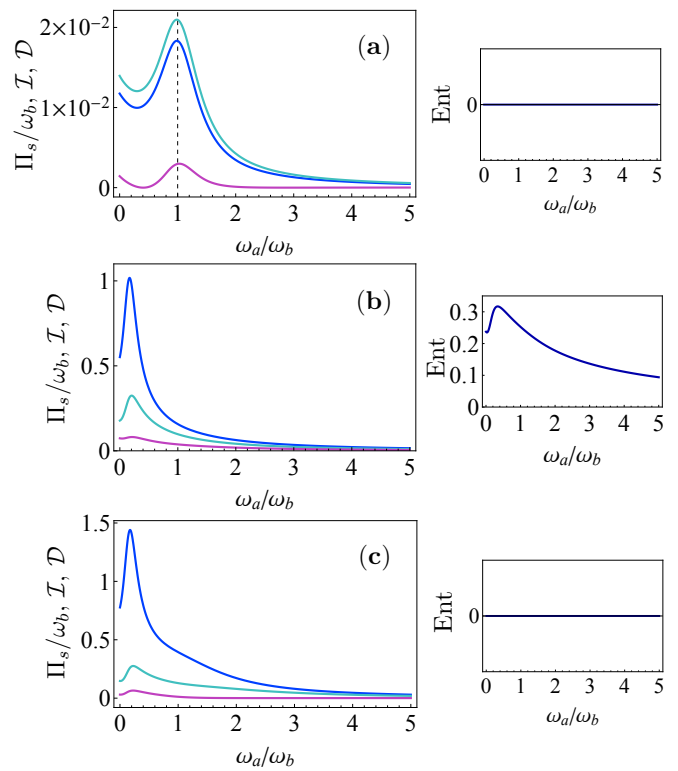


FIG. 6. Comparison between the steady-state (rescaled) entropy production rate Π_s (blue), the mutual information \mathcal{I} (green water), and the quantum discord \mathcal{D} (magenta) as a function of the ratio of the two frequencies ω_a/ω_b (left column) together with the entanglement between the mechanical and optical field (right column) quantified by the logarithmic negativity. (a) is for $G = 0.1\omega_b$, $\kappa_a = \kappa_b = 0.2\omega_b$ and $N_a = 0$ and $N_b = 1$; in (b) $g = 0.6\omega_m$, $\kappa_a = 0.2\omega_b$, $\kappa_b = 0.5\omega_b$, $N_a = N_b = 0$. Finally in (c) same parameters as (b) except for $N_b = 1$.

particular from panel (a) we notice a pronounced similarity. We can expand \mathcal{D} in series of the coupling strength (given the complexity of the expression we consider same initial thermal occupation $N_a = N_b = N$ and same rates κ) to get the following expression

$$\mathcal{D} = \frac{\Pi_s}{4\kappa_{\text{tot}}(N+1)} + \mathcal{O}(G^4), \quad (20)$$

where $\kappa_{\text{tot}} = 2\kappa$, and for completeness we also report the corresponding expression of Π_s

$$\Pi_s = \frac{2\kappa_{\text{tot}}G^2}{\kappa_{\text{tot}}^2 + (\omega_a + 1)^2}. \quad (21)$$

For small enough values of G the rate of irreversibility in the dynamics is proportional to the quantum correlations between the two modes. We point out that, at variance with Π_s and \mathcal{I} , the discord does depend on the initial number of thermal excitations. Moreover, a comparison between Eq. (18) and Eq. (20) shows that, when both the baths are in the ground state, we have $\mathcal{D} = \mathcal{I}/2$.

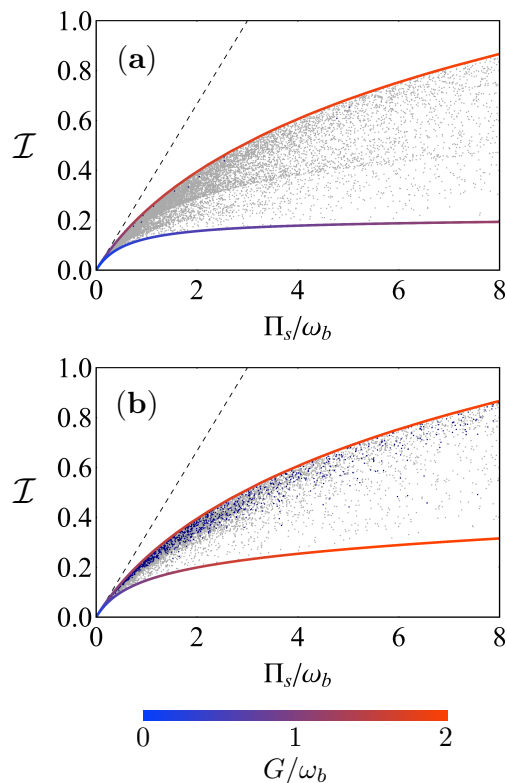


FIG. 7. Mutual information \mathcal{I} against the rescaled irreversible entropy production rate Π_s/ω_b for randomly generated states. Each point corresponds to a state obtained by a uniform sampling from $\omega_a \in [0, 3\omega_b]$, $G \in [0, 2\omega_b]$, and either $N_{a,b} \in [0, 10]$ (a) or $N_{a,b} \in [0, 1]$ (b). Dissipation rates are kept fixed at $\kappa_a = 0.5\omega_b$, $\kappa_b = \omega_b$. Points corresponding to separable states are shown in gray, while entangled states are marked in blue. The upper and lower bounds are parametric curves obtained by varying the coupling G from $G_{\min} = 0$ (blue) to a maximum value $G_{\max} = 2\omega_b$ (red). The dashed straight line corresponds to $\mathcal{I} = \Pi_s/(2\kappa_{\text{tot}})$.

D. Full comparison between irreversibility and correlations

To better understand the relationship between Π_s and the correlations \mathcal{I} and \mathcal{D} , we proceed by randomly generating non-equilibrium steady states and evaluating the quantities of interest. The resulting plots are shown in Figs. 7 and 8, where we have considered uniform distributions for the dimensionless frequency $\omega_a \in [0, 3]$, coupling values $G \in [0, 2]$, and either $N_{a,b} \in [0, 10]$, for the case shown in panel (a), or $N_{a,b} \in [0, 1]$ in (b). The value of the dissipation rates has been kept fixed and set to $\kappa_a = 0.5$ and $\kappa_b = 1$. Furthermore, points corresponding to separable states are shown in gray, while entangled states are marked in blue. From Fig. 7, which compares Π_s and \mathcal{I} , we see that all the randomly-generated points lie between two monotonically non-decreasing curves. Equivalently stated, for a given degree of irreversibility Π_s , the total amount of correlations is both upper and

lower bounded. The upper bound turns out to be attained by oscillators having the same frequency and placed in contact with baths at the same temperature. For such a maximally symmetric configuration for analytical expressions of both Π_s and \mathcal{I} (the latter only for $\kappa_a = \kappa_b$) have been provided in Eq. (11) and Eq. (19), respectively. On the other hand, the lower bound corresponds to states having $\omega_a = 0$ and maximum imbalance in the initial populations, with all the excitations in the mode \hat{b} , i.e., $N_a = 0$ and $N_b = N_{\max}$ [with $N_{\max}=10$ panel (a) and $N_{\max} = 1$ in (b)]. The class of states saturating the lower bound is therefore highly non symmetric, with the oscillator \hat{a} frozen in the stationary state and its bath in the ground state.

In Fig. 7 parametric curves with respect to the coupling G are shown, for both the upper and the lower bounds, which go from $G_{\min} = 0$ (blue), to a maximum value $G_{\max} = 2$ (red). The linear relation expressed in Eq. (18) is stressed by a dashed line, and we can see that is only accurate in a neighborhood of the origin of the plane where typically states with small coupling lie. In particular, it can be checked that the configuration achieving the lower bound is stable for any value of the coupling G and achieves an asymptote for high values of Π_s , which corresponds to the limit of infinite coupling. This value can be computed analytically and reads

$$\mathcal{I}_{\min}^{\infty} = \frac{1}{2} \log \left[\frac{(\kappa_a + 2\kappa_b)(2\kappa_a^3 + \kappa_b + 8\kappa_a^2\kappa_b + 8\kappa_a\kappa_b^2 + \kappa_b^3)}{\kappa_a\kappa_b(1 + \kappa_b^2)} \right]. \quad (22)$$

In Fig. 7 (b) we have considered lower values of the maximum number of initial thermal excitations allowed. While as we know this does not affect the upper bound, the separable/entangled nature of the stationary states gets drastically affected, with now many more entangled states generated by the dissipative process. We also notice that entangled states are denser in the region close to the upper bound. This fact is somehow expected since highly quantum-correlated states typically have high values of mutual information (classical plus quantum correlations).

In Fig. 8 we present a similar analysis for the Rényi-2 discord. The dashed straight line corresponds to $\mathcal{D} = \Pi_s/(4\kappa_{\text{tot}})$ and, as explained above, accurately describes states with $N_a = N_b = 0$ and vanishing values of the coupling. In the small-coupling limit, it can be verified that the optimal measurement to be implemented on the mode \hat{b} (the one that saturates Eq. (17) and yields the quantum discord) is heterodyne detection (see Appendix D). On the other hand, the upper bound turns out to be attained by states having $\omega_a = 0$ and $N_a = N_b = 0$, i.e. with both the oscillators initially in the ground state. On the other hand, whenever $N_b = 0$, homodyne detection turns out to be the optimal measurement.

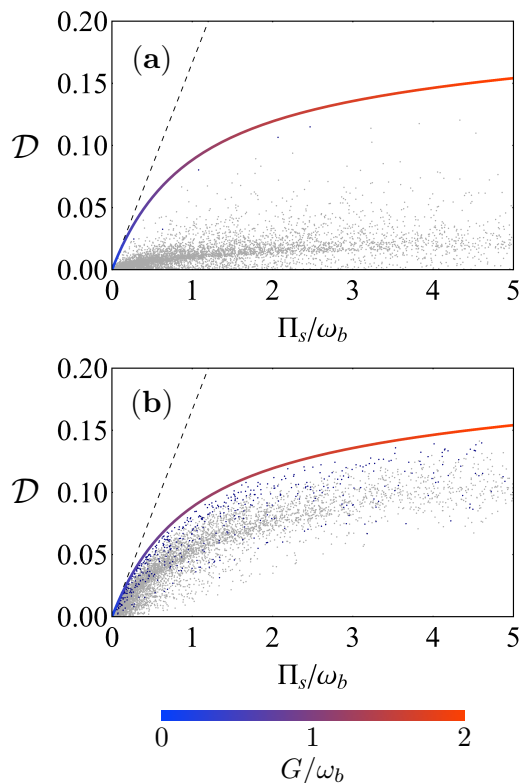


FIG. 8. Quantum discord \mathcal{D} against the rescaled irreversible entropy production rate Π_s/ω_b for randomly generated states. Detail of the generation are the same as in Fig. 7. The dashed straight line corresponds to $\mathcal{D} = \Pi_s/(4\kappa_{\text{tot}})$.

IV. IRREVERSIBILITY AND CORRELATIONS IN AN OPTOMECHANICAL SYSTEM

In this Section we particularize our findings to characterize irreversibility in a quantum optomechanical system. Optomechanical-like devices allow for the quantum-coherent manipulation of mesoscopic mechanical systems [30–33]. As such, they have recently attracted some attention as a platform where to investigate thermodynamics in the quantum regime and as a well-versed candidate to realize quantum thermal machines [34–39].

The system we consider is an optomechanical cavity of length L externally pumped by a laser having frequency ω_0 and strength $\mathcal{E} = \sqrt{2P\kappa/\hbar\omega_0}$, where P is the incident laser power and κ is the cavity decay rate. A mechanical mode of frequency ω_m is coupled to the cavity mode due to radiation-pressure interaction. The Hamiltonian of the system (in a rotating frame at the frequency of the external pump) reads [7]

$$\hat{H}_0 = \hbar\Delta_0\hat{a}^\dagger\hat{a} + \frac{\hbar\omega_m}{2}(\hat{q}^2 + \hat{p}^2) - \hbar g_0\hat{a}^\dagger\hat{a}\hat{q} + i\hbar\mathcal{E}(\hat{a}^\dagger - \hat{a}), \quad (23)$$

where $\Delta_0 = \omega_c - \omega_0$ is the cavity-pump detuning, \hat{q} and \hat{p} are the mechanical dimensionless quadratures, and the strength of the radiation pressure interaction is quan-

tified by the single-photon coupling rate $g_0 = \frac{\omega_c x_{\text{zpf}}}{L}$, where $x_{\text{zpf}} = \sqrt{\hbar/m\omega_m}$ is the zero-point term of the mechanical resonator. The dynamics of the system is also influenced by the presence of the environment. The mechanical mode is affected by the zero-mean Brownian stochastic force $\hat{\xi}(t)$, which for high mechanical quality factors can be taken to be Markovian, and experiences dissipation at a rate γ_m . The intra-cavity field couples to the outside vacuum electromagnetic field, described by delta-correlated input noise \hat{a}^{in} . The noise vector entering the equations of motion is given by $\hat{N} = (0, \hat{\xi}, \sqrt{2\kappa}\hat{X}^{\text{in}}, \sqrt{2\kappa}\hat{Y}^{\text{in}})^T$. For a strong driving, provided that the system remains in a stable regime, the cavity field reaches a steady value of the amplitude $\langle \hat{a} \rangle_s = \alpha$, and one can consider small quantum fluctuations around the classical steady state. This procedure leads to a linearized interaction $\hat{H}_I = 2\hbar g \delta\hat{q} \delta\hat{X}$ between the mechanical ($\delta\hat{q}$) and optical ($\delta\hat{X}$) fluctuation operators and an enhanced optomechanical coupling $g = \frac{\sqrt{2}g_0|\alpha|}{\sqrt{\kappa^2 + \Delta^2}}$, where $\Delta = \Delta_0 - \frac{g_0^2|\alpha|^2}{\omega_m}$ [40]. Therefore, the driven-dissipative optomechanical system matches our abstract model of linearly coupled quantum oscillators, provided that the oscillator \hat{a} is identified with the quantum fluctuation of cavity field, and \hat{b} with the annihilation operator of the mechanical fluctuation. Formally the correspondence is realized by replacing the vector $\hat{u} = (\hat{q}_a, \hat{p}_a, \hat{q}_b, \hat{p}_b)^T$ by the vector of zero-mean fluctuation operators $(\delta\hat{q}, \delta\hat{p}, \delta\hat{X}, \delta\hat{Y})^T$ and by the following identification: $\omega_a = \Delta$, $\omega_b = \omega_m$, $G = 2g$, $\kappa_a = \kappa$, $\kappa_b = \gamma_m$, $N_b = N$ and $N_a = 0$. In the following analysis we will employ dimensionless quantities. All the frequencies involved are understood to be in units of the mechanical frequency ω_m , except for the captions of the figures.

One main difference with respect to the generic case of Section I is that the effective frequency of the optical oscillator can now be tuned, and this enables us to explore the range of negative detunings, which was previously forbidden. In Fig. 9 (a) and (b) we display the behavior of the the optical and mechanical contributions to the entropy production μ_a and μ_b against the detuning, whence we see that for small values of the coupling the system is stable also in the blue-detuned region $\Delta < 0$. For large values of the detuning $|\Delta| \gg 1$ the two oscillators are effectively decoupled and each of them comes to equilibrium with its own bath, thus leading to vanishing Π_s , in agreement to what observed in Sec. II. The chosen values of the parameters place the system in the resolved sideband regime. This is reflected in the behavior of the entropy production rate, with both contributions μ_a and μ_b clearly peaked at the two mechanical sidebands. For frequencies $\Delta \approx 1$ the dominant beam splitter interaction $\hat{H}_I \propto \delta\hat{a}^\dagger\delta\hat{b} + \delta\hat{a}\delta\hat{b}^\dagger$ determines an enhanced heat transport, necessarily accompanied by an entropy increase. From Fig. 9 (a) we see that the peak is even more pronounced in the amplification regime. Indeed, for $\Delta \approx -1$ the two-mode squeezing like interac-

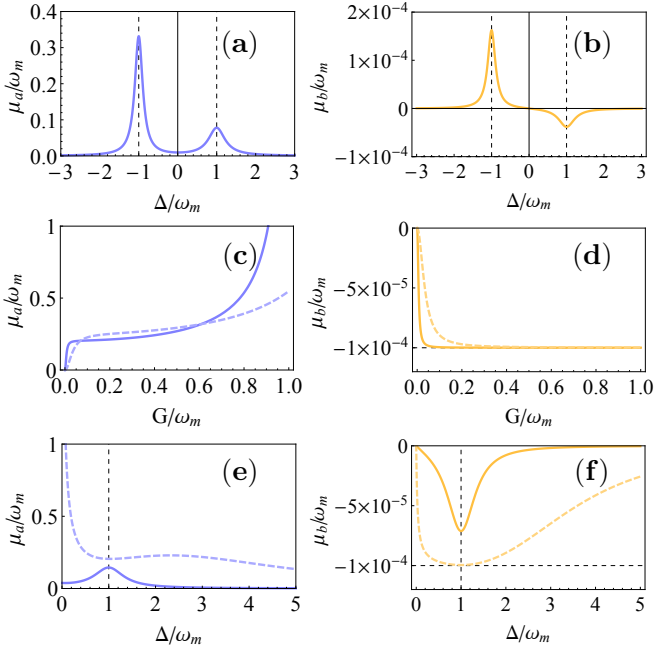


FIG. 9. Top row: Rescaled optical (a) and mechanical (b) contributions to the entropy production rate against the detuning Δ/ω_m , for $g = 0.005\omega_m$, $\kappa = 0.2\omega_m$, $\gamma_m = 10^{-4}\omega_m$ and $N = 10^3$. Middle row: optical (c) and mechanical (d) contributions against the rescaled coupling g/ω_m ; solid curves correspond to $\Delta = \omega_m$, while dashed ones to $\Delta = 2\omega_m$. Other parameters are $\kappa = 0.2\omega_m$, $\gamma_m = 10^{-4}\omega_m$ and $N = 10^3$. Panels (e) and (f) are obtained for the same values as (a) and (b), except for the coupling which is given by $g = 0.01\omega_m$ (solid curves) and $g = 0.1\omega_m$ (dashed curves).

tion $\hat{H}_I \propto \delta\hat{a}^\dagger\delta\hat{b}^\dagger + \delta\hat{a}\delta\hat{b}$ prevails, causing an exponential growth of the energies stored in the oscillators and inducing strong correlations between the two (EPR-like entanglement, in the infinite energy limit). And from our analysis it follows that the entropy production must correspondingly increase. On the other hand, from Fig. 9 (b) we see that μ_b changes sign, which clearly captures the heating/cooling of the mechanical resonator. We can thus conclude that the behavior of Π_s and its contributions gives a full thermodynamical account of both the amplification and cooling regimes.

In Fig. 9 (c) and (d) $\mu_{a,b}$ are shown as a function of the coupling, for different values of Δ . The Routh-Hurwitz criterion determines the limiting value of the coupling (for a given detuning) beyond which the system is no longer stable [41]. We can see that μ_a is divergent when approaching that value, which overall makes Π_s diverge. On the other hand, μ_b tends to an asymptotic value which, depending on the detuning Δ , is approached for smaller or bigger coupling strengths. As expected, for $\Delta = 1$ [solid line in panel (d)] the optimal working point for cooling is attained, which is manifested by the fact that the limiting value of μ_b is approached for the smallest value of the coupling.

Finally, in Fig. 9 (e) and (f) we plot μ_a and μ_b

for higher values of the optomechanical coupling. The blue-detuned region is now excluded because the semi-classical steady state is no longer stable. μ_a and μ_b increase (in absolute value) for increasing values of the coupling, which accounts for the fact that the stronger the interaction between the oscillators the more irreversible the corresponding stationary process. In particular for $g = 0.1$ the multi-photon quantum cooperativity is $\mathcal{C} = 4g^2/\kappa\gamma N = 50$, which places the system deeply in the quantum regime. The main feature to be noticed in plot (e) is that the behavior of the entropy production changes qualitatively: for $g = 0.01$ μ_a still displays a maximum at the mechanical sideband, while for $g = 0.1$ we see a divergence close to resonance and a local minimum around $\Delta = 1$. On the other hand in panel (f) we see that the minimum always occurs at $\Delta = 1$, the only difference being in its depth and its width.

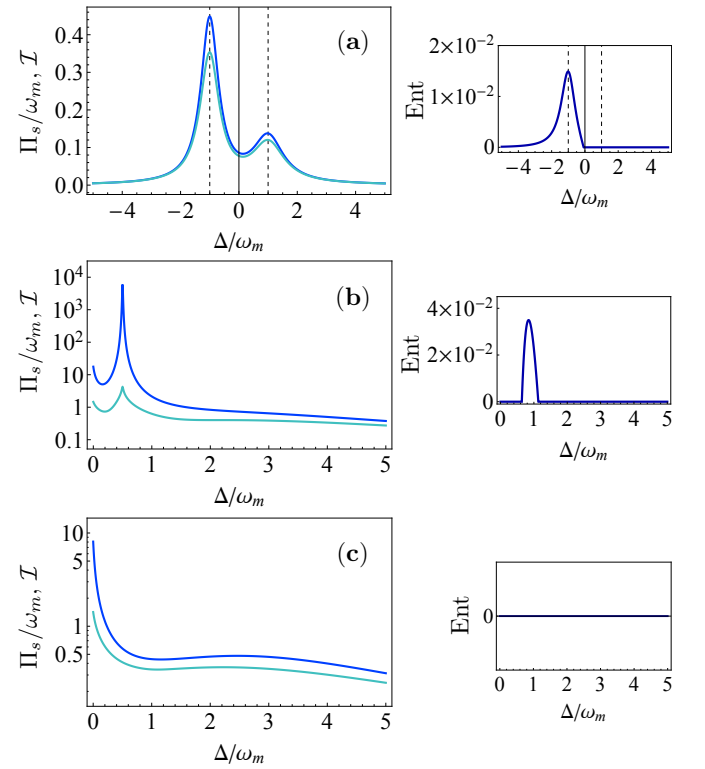


FIG. 10. Comparison between the steady-state entropy production rate Π_s (blue) and mutual information \mathcal{I} (green water) as a function of the rescaled detuning Δ/ω_m (left) together with the entanglement between the mechanical and optical field (right) quantified by the logarithmic negativity. (a) is for $g = 0.1\omega_m$, $\gamma_m = 10^{-2}\omega_m$, $\kappa = 0.5\omega_m$ and $N = 10$; in (b) logarithmic plot with same parameters but strong coupling $g = \omega_m$. Finally in (c) same parameters as (a) except for $\gamma_m = 10^{-4}\omega_m$ and $N = 10^3$.

In Fig. 10 we compare the entropy production rate Π_s to the correlations established by the optomechanical interaction, as quantified by the mutual information \mathcal{I} . In panel (a) we have considered a small coupling ($g = 0.1$) and a very low initial occupation of the me-

chanical oscillator ($N = 10$). The two figures of merit are extremely close to each other for the whole range of detunings. Indeed, in this limit Eq. (18) safely applies. The two-mode squeezing, which prevails in the region $\Delta \approx -1$, is an explicitly entangling operation that establishes strong quantum correlations, thus leading to a sudden increase of both \mathcal{I} and Π_s that are strongly peaked at the mechanical sideband. This is further confirmed by the presence of steady-state entanglement (quantified by the logarithmic negativity) in the blue detuned region, as shown in the right box. In panel (b) the system is in the strong coupling regime, which causes $t\Pi_s$ to increase exponentially with respect to the total amount of correlations. However, even if no analytical relation can be grasped in this case, from the plot is clear the similarity between the two figures of merit persists. Finally, in (c) we consider more realistic values of the parameters $N = 10^3$ $g = 0.1$. Also for such a high imbalance in the number of excitations it is possible to see that \mathcal{I} and Π_s bear the same features, in particular being both maximum at resonance ($\Delta = 0$).

Expanding up to second order in G and neglecting γ we obtain the following expression for the entropy production rate

$$\Pi_s = \frac{2\kappa G^2}{2N+1} \left(\frac{N^2}{(\Delta-1)^2 + \kappa^2} + \frac{(N+1)^2}{(\Delta+1)^2 + \kappa^2} \right) + \mathcal{O}(g^4). \quad (24)$$

V. CONCLUSIONS

With quantum-limited control extending over systems of increasing size and complexity, the development of a dynamical theory of irreversible heat exchange for mesoscopic quantum systems undergoing finite-time transformation is fully due. In this work we have taken a step in this direction, by quantitatively assessing the irreversible entropy generated in an interacting quantum system by a stationary dissipative process. First, we presented two alternative expressions for the stationary entropy produc-

tion rate which relate in a simple way the irreversibility of the process to the features of the open system dynamics. Second, we established a connection between the entropy production rate and the amount of total and quantum correlations shared by the two subsystems. In order to do so, we found instrumental to quantify correlations by means of the Rényi-2 entropy. We showed how the onset of irreversibility, which quantifies the departure from quasi-static reversible transformations, and the amount of correlations established by a process must be view as complementary features. Our results provide, for instance, a clear picture of the irreversibility taking place in a cavity optomechanical system. There, the entropy production rate turns out to be a very informative figure of merit, accounting for both sideband cooling and amplification regimes.

Possible applications of our work concern the optimization of quantum thermal machines operating at the steady state. For example, the model we considered can be taken as an instance of an autonomous quantum thermal machine that generates steady state quantum correlations being only powered by heat [42], in which case our study accounts for the performances of such a machine. Furthermore, we plan to extend our analysis to a time-dependent scenario. This would enable to incorporate relaxation towards equilibrium as well as time-dependent driving and feedback, with the goal of engineering genuinely out-of-equilibrium transformations in interacting quantum systems with the minimal generation of entropy.

ACKNOWLEDGEMENTS

This work was supported by the UK EPSRC (EP/L005026/1 and EP/J009776/1), the John Templeton Foundation (grant ID 43467) and the EU Collaborative Project TherMiQ (Grant Agreement 618074). Part of this work was supported by COST Action MP1209 “Thermodynamics in the quantum regime”.

-
- [1] R. C. Tolman and P. C. Fine, On the Irreversible Production of Entropy, *Rev. Mod. Phys.* **20**, 51 (1948).
 - [2] M. Esposito and C. Van den Broeck, Three faces of the second law: I. Master equation formulation, *Phys. Rev. E* **82**, 011143 (2010).
 - [3] R. Kosloff and A. Levy, Quantum Heat Engines and Refrigerators: Continuous Devices, *Annu. Rev. Phys. Chem.* **65**, 365 (2014).
 - [4] L. Henderson, V. Vedral, Classical, quantum and total correlations, *J. Phys. A* **34** (35), 6899.
 - [5] K. Modi, A. Brodutch, H. Cable, T. Paterek and V. Vedral, The classical-quantum boundary for correlations: discord and related measures, *Rev. Mod. Phys.* **84**, 1655 (2012).
 - [6] M. Huber, M. Perarnau-Llobet, K. V. Hovhannisyan, P. Skrzypczyk, C. Klöckl, N. Brunner and A. Acín, Thermodynamic cost of creating correlations, *New J. Phys.* **17** 065008 (2015).
 - [7] M. Aspelmeyer, T. Kippenberg, and F. Marquardt, Cavity optomechanics, *Rev. Mod. Phys.* **86**, 1391 (2014).
 - [8] H. B. Callen, *Thermodynamics and an introduction to thermostatistics* (Wiley, New York, 1985).
 - [9] I. Prigogine, *Introduction to thermodynamics of irreversible processes*, (John Wiley & Sons, 1968).
 - [10] U. Seifert, Stochastic thermodynamics fluctuation theorems and molecular machines, *Rep. Prog. Phys.* **75**, 126001 (2012).
 - [11] C. Jarzynski, Equalities and Inequalities: Irreversibility and the Second Law of Thermodynamics at the Nanoscale,

- Annu. Rev. Condens. Matter Phys.* **2**, 329 (2011).
- [12] C. Van den Broeck and M. Esposito, Three faces of the second law: II. Fokker-Planck formulation, *Phys. Rev. E* **82**, 011144 (2010).
- [13] J. M. R. Parrondo, C. Van den Broeck and R. Kawai, Entropy production and the arrow of time, *New J. Phys.* **11** 073008 (2009).
- [14] U. Seifert, Entropy Production along a Stochastic Trajectory and an Integral Fluctuation Theorem, *Phys. Rev. Lett.* **95**, 040602 (2005).
- [15] H. Spohn, J. L. Lebowitz, Irreversible thermodynamics for quantum systems weakly coupled to thermal reservoirs, *Adv. Chem. Phys.* **38**, 109 (1978).
- [16] S. Deffner and E. Lutz, Nonequilibrium entropy production for open quantum systems, *Phys. Rev. Lett.* **107**, 140404 (2011).
- [17] M. Esposito, K. Lindeberg, and C. Van den Broeck, Entropy production as correlation between system and reservoir, *New J. Phys.*, **12** 013013 (2010).
- [18] J. V. Koski, T. Sagawa, O-P. Saira, Y. Yoon, A. Kutvonen, P. Solinas, M. Möttönen, T. Ala-Nissila and J. P. Pekola, Distribution of entropy production in a single electron box, *Nature Phys.* **9**, 644 (2013).
- [19] C. Tietz, S. Schuler, T. Speck, U. Seifert, and J. Wrachtrup, Measurement of Stochastic Entropy Production, *Phys. Rev. Lett.* **97**, 050602 (2006).
- [20] J. Gieseler, R. Quidant, C. Dellago and L. Novotny, Dynamic relaxation of a levitated nanoparticle from a non-equilibrium steady state, *Nature Nanotech.* **9**, 358 (2014).
- [21] M. Brunelli, L. Fusco, R. Landig, W. Wiecezorek, J. Hoelscher-Obermaier, G. Landi, F.L. Semião, A. Ferraro, N. Kiesel, T. Donner, G. De Chiara, and M. Paternostro, Measurement of irreversible entropy production in mesoscopic quantum systems out of equilibrium, arXiv:1602.06958 (2016).
- [22] C. Weedbrook, S. Pirandola, R. García-Patrón, N. J. Cerf, T. C. Ralph, J. H. Shapiro and S. Lloyd, Gaussian quantum information, *Rev. Mod. Phys.* **84**, 621 (2012).
- [23] A. Ferraro, S. Olivares, and M. G. A. Paris, *Gaussian States in Quantum Information* (Bibliopolis, Napoli, 2005).
- [24] T. Tomé, and M. J. de Oliveira, Entropy production in irreversible systems described by a Fokker-Planck equation, *Phys. Rev. E* **82**, 021120 (2010).
- [25] G. T. Landi, T. Tomé, and M. J. de Oliveira, Entropy production in linear Langevin systems, *J. Phys. A: Math. Theor.* **46**, 395001 (2013).
- [26] R. E. Spinney and I. J. Ford, Entropy production in full phase space for continuous stochastic dynamics, *Phys. Rev. E* **85**, 051113 (2012).
- [27] A. Asadian, D. Manzano, M. Tiersch, and H. J. Briegel, Heat transport through lattices of quantum harmonic oscillators in arbitrary dimensions *Phys. Rev. E* **87**, 012109 (2013).
- [28] V. Vedral, The role of relative entropy in quantum information theory, *Rev. Mod. Phys.* **74**, 197 (2002).
- [29] G. Adesso, D. Girolami, and A. Serafini, Measuring Gaussian quantum information and correlations using the Rényi entropy of order 2, *Phys. Rev. Lett.* **109**, 190502 (2012).
- [30] A. Schliesser, R. Rivière, G. Anetsberger, O. Arcizet, and T. Kippenberg, Resolved-sideband cooling of a micromechanical oscillator, *Nature Phys.* **4**, 415 (2007).
- [31] J. Chan, T. P. Mayer Alegre, A. H. Safavi-Naeini, J. T. Hill, A. Krause, S. Gröblacher, M. Aspelmeyer, and O. Painter, Laser cooling of a nanomechanical oscillator into its quantum ground state, *Nature* **478**, 89 (2011).
- [32] J. D. Teufel, T. Donner, Dale Li, J. W. Harlow, M. S. Allman, K. Cicak, A. J. Sirois, J. D. Whittaker, K. W. Lehnert and R. W. Simmonds, Sideband cooling of micromechanical motion to the quantum ground state, *Nature* **475**, 359 (2011).
- [33] E. Verhagen, S. Deléglise, S. Weis, A. Schliesser and T. J. Kippenberg, Quantum-coherent coupling of a mechanical oscillator to an optical cavity mode, *Nature* **482**, 63 (2012).
- [34] K. Zhang, F. Bariani, and P. Meystre, Quantum optomechanical heat engine, *Phys. Rev. Lett.* **112**, 150602 (2014).
- [35] M. Brunelli, A. Xuereb, A. Ferraro, G. De Chiara, N. Kiesel, and M. Paternostro, Out-of-equilibrium thermodynamics of quantum optomechanical systems, *New J. Phys.* **17**, 035016 (2015).
- [36] C. Elouard, M. Richard, A. Auffèves, Reversible work extraction in a hybrid opto-mechanical, *New J. Phys.* **17**, 055018 (2015).
- [37] A. Mari, A. Farace, V. Giovannetti, Quantum optomechanical piston engines powered by heat, *J. Phys. B* **48**, 175501 (2015).
- [38] D. Gelbwaser-Klimovsky, G. Kurizki, Work extraction from heat-powered quantized optomechanical setups, *Sci. Rep.* **5**, 7809 (2015).
- [39] M. Mitchison, M. Huber, J. Prior, M. P. Woods, and M. B. Plenio, Autonomous quantum thermal machines in atom-cavity systems, arXiv:1603.02082 (2016).
- [40] M. Paternostro, S. Gigan, M. S. Kim, F. Blaser, H. R. Böhm, and M. Aspelmeyer, Reconstructing the dynamics of a movable mirror in a detuned optical cavity, *New J. Phys.* **8**, 107 (2006).
- [41] A. Hurwitz, *Selected papers on Mathematical trends in control theory* (ed R. Bellman & R. Kalaba, New York, Dover, 1964).
- [42] J. B. Brask, G. Haack, N. Brunner and M. Huber, Autonomous quantum thermal machine for generating steady-state entanglement, *New J. Phys.*, **17**, 113029 (2015).

APPENDIX

Appendix A: Quantifying information by the Rényi-2 entropy

In this Appendix we motivate the adoption of correlation measures based on the Rényi-2 entropy. Let us consider a n -mode bosonic state ρ and let $\mathcal{W}_\rho(X)$ be the Wigner function associated to it, with $X \in \mathbb{R}^{2n}$. If $\mathcal{W}_\rho(X)$ is a legitimate probability distribution we can compute its Shannon entropy $S(\mathcal{W}_\rho) = -2^{-n} \int_{\mathbb{R}^{2n}} d^{2n}X \mathcal{W}_\rho(X) \log \mathcal{W}_\rho(X)$. In particular, if the state is a (zero-mean) Gaussian state with covariance matrix σ , namely a state whose Wigner function has the form

$$\mathcal{W}_\sigma(X) = \frac{1}{\pi^n \sqrt{\det \sigma}} e^{-\frac{1}{2} X^T \sigma^{-1} X}, \quad (25)$$

its Shannon entropy $S(\mathcal{W}_\sigma) \equiv S_\sigma$ can be explicitly evaluated and is given by

$$S_\sigma = \frac{1}{2} \log \det \sigma + n \log \pi e. \quad (26)$$

Interestingly, for Gaussian states this expression coincides, up to an additive constant, with the generalized Rényi entropy of order 2. The Rényi- α entropy is defined as $S_\alpha(\rho) = (1 - \alpha)^{-1} \log \text{Tr}[\rho^\alpha]$ with $\alpha \geq 0$, and is a generalization of the usual entropy functional (one can indeed show that in the limit $\alpha \rightarrow 1$ the von Neumann entropy $S_1 = -\text{Tr} \rho \log \rho$ is recovered). When $\alpha = 2$ the Rényi entropy takes the particularly simple expression $S_2(\rho) = -\log \text{Tr} \rho^2$, namely minus the logarithm of the purity of the state ρ . For Gaussian states the purity can be easily evaluated as $\text{Tr} \rho^2 = (\pi/2)^n \int_{\mathbb{R}^{2n}} d^{2n} X \mathcal{W}_\sigma^2(X) = 2^{-n} (\det \sigma)^{-1/2}$, yielding $S_2 = \frac{1}{2} \log \det \sigma + n \log 2$. By comparing the latter expression with Eq. (26) we thus have

$$S_\sigma = S_2 + n \log \frac{\pi}{2} e, \quad (27)$$

which proves our statement.

In Ref. [A1] the strong subadditivity of S_2 for Gaussian states has been proved, and measures of both the mutual information (\mathcal{I}_2) and the quantum discord (\mathcal{D}_2) built upon it have been introduced. We must stress that the adoption of correlation measures based on the Von Neumann entropy S_1 is perfectly legitimate, and actually standardly employed; for bipartite Gaussian states analytical expressions of both the mutual information (\mathcal{I}_1) and the quantum discord (\mathcal{D}_1) are available [A2–A4]. However, while these require the knowledge of the full symplectic spectrum, those based on the Rényi-2 entropy only involve the local and global purities of the system, thus leading to much easier expressions. In our analysis we have adopted \mathcal{I}_2 and \mathcal{D}_2 to quantify the amount of total and quantum correlations, respectively. However, in order to ascertain the consistency of our choice, we compared \mathcal{I}_2 (\mathcal{D}_2) and \mathcal{I}_1 (\mathcal{D}_1) for the coupled oscillators in the stationary state, finding that they display the very same behavior, with \mathcal{I}_2 (\mathcal{D}_2) in general assuming slightly smaller values than \mathcal{I}_1 (\mathcal{D}_1).

Appendix B: Derivation of the stationary entropy production rate Eq. (6)

In this Appendix we provide explicit expressions for the entropy production rate $\Pi(t)$ and the entropy flux $\Phi(t)$ appearing in Eq. (2). In particular, we derive the expression for steady-state entropy production rate $\Pi_s = -\dot{\Phi}_s$ shown in Eq. (6). The entropy is quantified by means of the Shannon entropy of the Wigner distribution of the state Eq. (26). Since we are interested in entropy rates, the additive constant in Eq. (27) plays no role, so that we can remove the subscripts and denote the entropy just by

S . The following derivation is based on Ref. [A5], where however classical stochastic processes were considered.

The dynamics of the system, as introduced in Sec. I, has been described as the solution of the quantum Langevin equations for the vector $\hat{u} = (\hat{q}_a, \hat{p}_a, \hat{q}_b, \hat{p}_b)^T$. It can be equivalently expressed in terms of a Fokker-Planck equation for the Wigner function $\mathcal{W}(u, t)$

$$\partial_t \mathcal{W} = -\text{div} J(u, t), \quad (28)$$

where $u = (q_a, p_a, q_b, p_b)^T$ is a point in the phase space and we have introduced the probability current vector

$$J(u, t) = Au\mathcal{W}(u, t) - \frac{1}{2}D\partial_u\mathcal{W}(u, t). \quad (29)$$

The drift and diffusion matrices A and D appearing in Eq. (29) are defined in Sec. I, and by ∂_u we mean the phase-space gradient. By introducing the time-reversal operator $E = \text{diag}(1, -1, 1, -1)$, the dynamical variables can be split according to their symmetry. The drift matrix A is accordingly divided in an irreversible component $A^{\text{irr}}(Eu) = E(A^{\text{irr}}u)$ which is even with respect to time reversal, and a reversible one $A^{\text{rev}}(Eu) = -E(A^{\text{rev}}u)$, which is odd [A6]. They can be constructed as $A^{\text{irr}} = \frac{1}{2}(A + EAE^T)$ and $A^{\text{rev}} = \frac{1}{2}(A - EAE^T)$ and explicitly read

$$A^{\text{irr}} = \text{diag}(-\kappa_a, -\kappa_a, -\kappa_b, -\kappa_b), \quad (30)$$

and

$$A^{\text{rev}} = \begin{pmatrix} 0 & \omega_a & 0 & 0 \\ -\omega_a & 0 & G & 0 \\ 0 & 0 & 0 & \omega_b \\ G & 0 & -\omega_b & 0 \end{pmatrix}, \quad (31)$$

while $D \equiv D^{\text{irr}}$. This separation induces a similar splitting in the probability current $J(u, t) = J^{\text{rev}}(u, t) + J^{\text{irr}}(u, t)$, where

$$J^{\text{rev}}(u, t) = A^{\text{rev}}u\mathcal{W}(u, t), \quad (32)$$

and

$$J^{\text{irr}}(u, t) = A^{\text{irr}}u\mathcal{W}(u, t) - \frac{1}{2}D\partial_u\mathcal{W}(u, t). \quad (33)$$

We notice that, given the form of Eq. (31), the reversible part of the probability current is divergence-less, i.e., $\text{div} J^{\text{rev}}(u, t) = \mathcal{W}(u, t) \text{Tr}[\partial_u(A^{\text{rev}}u)] = 0$.

The detailed balance condition is retrieved by demanding $J_{\text{eq}}(u) \equiv 0$ and noting that the corresponding distribution $\mathcal{W}_{\text{eq}}(u)$ is left unchanged by time-reversal, i.e. $\mathcal{W}_{\text{eq}}(Eu) = \mathcal{W}_{\text{eq}}(u)$. Together these conditions correspond to microscopic reversibility and in this case the system's covariance matrix reduces to $\sigma_{\text{eq}} = (N_a + 1/2)\mathbb{1}_a \oplus (N_b + 1/2)\mathbb{1}_b$, thus describing two locally thermal states. On the other hand, when $\text{div} J_s(u) \equiv 0$ the system is found in a non-equilibrium stationary state. The two oscillators are now interacting with each other and detailed balance is broken because of the enforcement of non-equilibrium boundary conditions.

If we substitute Eq. (29) in the expression of the entropy rate we get

$$\frac{dS}{dt} = \frac{1}{4} \int du \operatorname{div} J(u, t) \log \mathcal{W}(u, t). \quad (34)$$

Then, invoking the divergence-less of J^{rev} we can write the integrand as $\operatorname{div} J(u, t) \log \mathcal{W}(u, t) = \operatorname{div} J^{\text{irr}}(u, t) \log \mathcal{W}(u, t) = \operatorname{div}(J^{\text{irr}}(u, t) \log \mathcal{W}(u, t)) - J^{\text{irr}}(u, t)^T \partial_u (\log \mathcal{W}(u, t))$ and we notice that the first term, when integrated, vanishes as a consequence of the Stokes theorem (we assume the probability density to be vanishing at the phase-space boundary). Therefore, the entropy rate is expressed as

$$\frac{dS}{dt} = -\frac{1}{4} \int du \frac{1}{\mathcal{W}(u, t)} J^{\text{irr}}(u, t)^T \partial_u \mathcal{W}(u, t). \quad (35)$$

Finally, by plugging in Eq. (33) we recover the splitting shown in Eq. (2) between entropy flux

$$\Phi(t) = -\frac{1}{4} \int du 2J^{\text{irr}}(u, t)^T D^{-1} A^{\text{irr}} u, \quad (36)$$

and entropy production rate

$$\Pi(t) = \frac{1}{4} \int du \frac{2}{\mathcal{W}(u, t)} J^{\text{irr}}(u, t)^T D^{-1} J^{\text{irr}}(u, t). \quad (37)$$

It has been possible to identify the last expression with the entropy production rate by virtue of its non-negativity, being Eq. (37) the integral of a quadratic form. Moreover, for a Gaussian state it is easy to show that the following relation holds, $\partial_u \mathcal{W}_\sigma(u, t) = -\mathcal{W}_\sigma(u, t) \sigma^{-1}(t) u$, so that irreversible component of probability current Eq. (33) becomes $J^{\text{irr}}(u, t) = \mathcal{W}_\sigma(u, t) (A^{\text{irr}} u + D) \sigma^{-1}(t) u$ and the integral in Eq. (37) can be explicitly carried out, giving

$$\Pi(t) = \frac{1}{2} \operatorname{Tr} [\sigma^{-1} D] + 2 \operatorname{Tr} [A^{\text{irr}}] + 2 \operatorname{Tr} [(A^{\text{irr}})^T D^{-1} A^{\text{irr}} \sigma]. \quad (38)$$

On the other hand, if we take the derivative of Shannon entropy of the Wigner function Eq. (25) we get $\frac{dS}{dt} = \frac{1}{2} \operatorname{Tr} [\sigma^{-1} \partial_t \sigma]$, where we applied the Jacobi formula to the derivative of the determinant. By inserting the evolution of the covariance matrix Eq. (5) we get

$$\frac{dS}{dt} = \frac{1}{2} \operatorname{Tr} [\sigma^{-1}(t) D] + \operatorname{Tr} [A^{\text{irr}}]. \quad (39)$$

By comparing the latter expression with Eq. (38) we can thus write

$$\Pi(t) = \frac{dS}{dt} - \Phi(t) \quad (40)$$

where

$$\Phi(t) = -\operatorname{Tr} [A^{\text{irr}}] - 2 \operatorname{Tr} [(A^{\text{irr}})^T D^{-1} A^{\text{irr}} \sigma(t)]. \quad (41)$$

In particular, when the system attains a stationary state we have $\Pi_s = -\Phi_s$, whose expression is given by

$$\Pi_s = \operatorname{Tr} [A^{\text{irr}}] + 2 \operatorname{Tr} [(A^{\text{irr}})^T D^{-1} A^{\text{irr}} \sigma_s]. \quad (42)$$

The latter is now in matrix form and the trace can be easily evaluated, giving

$$\Pi_s = 2\kappa_a \left(\frac{[\sigma_s]_{11} + [\sigma_s]_{22}}{2N_a + 1} - 1 \right) + 2\kappa_b \left(\frac{[\sigma_s]_{33} + [\sigma_s]_{44}}{2N_b + 1} - 1 \right) \quad (43)$$

which is the result displayed in Eq. (6).

Appendix C: Derivation of the equivalent expression Eq. (8)

In this Appendix we briefly show how to derive the expression for the stationary entropy production rate shown in Eq. (8). As shown in Sec. I, the steady-state covariance matrix obeys the Lyapunov equation

$$A\sigma_s + \sigma_s A^T = -D, \quad (44)$$

here rewritten for the sake of convenience, which imposes constraints between the elements of σ_s . Explicitly, the diagonal elements relative to the mode \hat{a} are re-expressed as

$$[\sigma_s]_{11} = \frac{1}{2} + N_a + \frac{\omega_a}{\kappa_a} [\sigma_s]_{12}, \quad (45)$$

$$[\sigma_s]_{22} = \frac{1}{2} + N_a + \frac{G[\sigma_s]_{23} - \omega_a [\sigma_s]_{12}}{\kappa_a}. \quad (46)$$

An analogous relation is found for the diagonal elements relative to the mode \hat{b} , upon the following substitutions $[\sigma_s]_{11} \rightarrow [\sigma_s]_{33}$, $[\sigma_s]_{12} \rightarrow [\sigma_s]_{34}$, $[\sigma_s]_{23} \rightarrow [\sigma_s]_{14}$, and $a \rightarrow b$. By plugging those expressions into Eq. (6), the required expression for $\mu_{a,b}$ Eq. (8) is easily found.

Appendix D: Rényi-2 Gaussian discord

In this Appendix we address more in detail the measure of discord based on the Rényi-2 entropy (here simply referred as \mathcal{D}), which has been used in the main text to quantify the amount of quantum correlations beyond entanglement in Gaussian states. In one Appendix of Ref. [A1] an explicit expression of the Rényi-2 discord for Gaussian states in standard form has been provided. However, both for the sake of completeness and because we adopt a different convention, in the following we show how to derive such expression. Moreover, we extend it to the case of generic two-mode Gaussian states, which is the relevant case for our investigation, expressing \mathcal{D} as a function of the symplectic invariants. The discord \mathcal{D} between modes \hat{a} and \hat{b} , when performing a measurement on \hat{b} , is defined as the following difference

$$\mathcal{D}(\sigma_{a|b}) = \mathcal{I}(\sigma_{a:b}) - \mathcal{J}(\sigma_{a|b}). \quad (47)$$

The first term on the right-hand side is the mutual information $\mathcal{I}(\sigma_{a:b}) = \frac{1}{2} \log \left(\frac{\det \sigma_a \det \sigma_b}{\det \sigma_{ab}} \right)$, while the second $\mathcal{J}(\sigma_{a|b}) = \sup_{\pi_b(X)} \{S(\sigma_a) - \int dX p_X S(\sigma_{a|X}^{\pi_b})\}$ quantifies the one-way classical correlations when performing

on \hat{b} a measurement $\hat{\pi}_b(X) \geq 0$, $\int dX \hat{\pi}_b(X) = \mathbb{1}$. If we focus on Gaussian measurements, we can consider a POVM of the form $\hat{\pi}_b(X) = \pi^{-1} \hat{D}_b(X) \hat{\rho}^{\pi_b} \hat{D}_b^\dagger(X)$ where $\hat{D}_b(X) = \exp(X\hat{b}^\dagger - X^*\hat{b})$ is the displacement operator and $\hat{\rho}^{\pi_b}$ a pure Gaussian state with covariance matrix $\gamma^{\pi_b} = R(\theta) \text{diag}(\lambda/2, \lambda^{-1}/2) R(\theta)^T$, where $\lambda \in [0, \infty]$ and $R(\theta) = \cos \theta \mathbb{1} - i \sin \theta \sigma_y$ is a rotation matrix. The conditional state of mode \hat{a} once the measurement $\hat{\pi}_b(X)$ has been performed turns out to be independent on the outcome of the measurement, i.e. $\sigma_{a|X}^{\pi_b} \equiv \sigma_a^{\pi_b}$. Its expression is given by $\sigma_a^{\pi_b} = \sigma_a - c_{ab}(\sigma_b + \gamma^{\pi_b})^{-1} c_{ab}^T$, where the block-form of the covariance matrix has been defined in Eq. (13). We thus have $\int dX p_X S(\sigma_{a|X}^{\pi_b}) = S(\sigma_a^{\pi_b})$ and the expression of one-way classical correlations reduces to

$$\mathcal{J}(\sigma_{a|b}) = \sup_{\pi_b} \frac{1}{2} \log \left(\frac{\det \sigma_a}{\det \sigma_a^{\pi_b}} \right). \quad (48)$$

$$E_{a|b}^{\min} = \frac{a^2(1-4b^2)^2 - 4ab(4b^2-1)(c^2+d^2) + 4\left(\sqrt{c^2d^2(-4ab^2+a+4bc^2)(-4ab^2+a+4bd^2)} + (4b^2+1)c^2d^2\right)}{(1-4b^2)^2}, \quad (52)$$

otherwise. It can be verified that the minimum in the first expression Eq. (51) is achieved by implementing homodyne detection on the mode \hat{b} , namely a projective measurement, e.g. along $\theta = 0$ with an infinite amount of squeezing $\lambda \rightarrow 0, \infty$. On the other hand, the minimum in the second expression of Eq. (52) is achieved by a positive operator-valued measurement.

The steady state σ_s of the dissipative dynamics Eq. (5)

$$E_{a|b}^{\min} = \begin{cases} \frac{(I_1 I_2 - I_3^2 + I_4) - \sqrt{\Lambda_-^2 - 2I_4 \Lambda_+ + I_4^2}}{2I_2} & \text{if } 4I_4(\Gamma_+ I_3^2 - I_4) + I_1(\Gamma_+ I_3^2 + 8I_2 I_4) < 4I_1^2 I_2^2, \\ \frac{I_1 - 4I_1 I_2 + 4(2I_3^2 - \Gamma_- I_4 + |I_3| \sqrt{I_1 - 4(\Gamma_- I_4 + \Lambda_-)})}{\Gamma_-^2} & \text{otherwise,} \end{cases} \quad (53)$$

where we defined the quantities $\Gamma_\pm = 1 \pm 4I_2$, and $\Lambda_\pm = I_1 I_2 \pm I_3^2$. The expression of the Rényi-2 discord for a

Accordingly, the Rényi-2 discord takes the form

$$\mathcal{D}(\sigma_{a|b}) = \frac{1}{2} \log(\det \sigma_b) - \frac{1}{2} \log(\det \sigma_{ab}) + \inf_{\pi_b} \frac{1}{2} \log(\det \sigma_a^{\pi_b}). \quad (49)$$

Let us first consider Gaussian states in standard form, i.e. those whose covariance matrix is given by

$$\sigma_{\text{std}} = \begin{pmatrix} a & 0 & c & 0 \\ 0 & a & 0 & d \\ c & 0 & b & 0 \\ 0 & d & 0 & b \end{pmatrix}. \quad (50)$$

For such states the minimization in Eq. (49) can be carried out analytically; if we denote $E_{a|b}^{\min} = \inf_{\theta, \lambda} \det \sigma_a^{\pi_b}$, and assuming $c > |d|$, explicit calculations show that its expression is given by

$$E_{a|b}^{\min} = a \left(a - \frac{c^2}{b} \right) \quad (51)$$

whenever the condition $[4ab^2d^2 - c^2(a + 4bd^2)] [4ab^2c^2 - d^2(a + 4bc^2)] < 0$, is satisfied and

is not in standard form. However, since the discord is invariant under local unitary operations, we can cast our state in standard form by means of a suitable set of local unitaries and then compute its discord. Equivalently, we can introduce the symplectic invariants $I_1 = \det \sigma_a$, $I_2 = \det \sigma_b$, $I_3 = \det c_{ab}$ and $I_4 = \det \sigma_{ab}$, and write the discord as a function of those. This leads us to the following expression for $E_{a|b}^{\min}$

generic two-mode Gaussian state is thus given by

$$\mathcal{D} = \frac{1}{2} \log \left(\frac{I_2 E_{a|b}^{\min}}{I_4} \right). \quad (54)$$

[A1] G. Adesso, D. Girolami, A. Serafini, Measuring Gaussian quantum information and correlations using the Rényi

entropy of order 2, *Phys. Rev. Lett.* **109**, 190502 (2012).

- [A2] A. Serafini, F. Illuminati, and S. De Siena, Symplectic invariants, entropic measures and correlations of Gaussian states, *J. Phys. B* **37**, L21 (2003).
- [A3] P. Giorda and M. G. A. Paris, Gaussian quantum discord, *Phys. Rev. Lett.* **105**, 020503 (2010).
- [A4] G. Adesso and A. Datta, Quantum versus classical correlations in Gaussian states, *Phys. Rev. Lett.* **105**, 030501 (2010).
- [A5] G. T. Landi, T. Tomé, and M. J. de Oliveira, Entropy production in linear Langevin systems, *J. Phys. A: Math. Theor.* **46**, 395001 (2013).
- [A6] R. E. Spinney and I. J. Ford, Entropy production in full phase space for continuous stochastic dynamics, *Phys. Rev. E* **85**, 051113 (2012).